Photochemical escape of oxygen from Mars using MAVEN in-situ measurements

Marko Gacesa[1,*], Rob Lillis[1], Ali Rahmati[1], Justin Deighan[2], Jane L. Fox[3], Yuni Lee[4], S. Bougher[4], J.-Y. Chaufray[5], Francois Leblanc[5], M. Combi[4], T. Cravens, and the MAVEN IUVS and NGIMS teams

[1]SSL, University of California, Berkeley, CA, USA [2]LASP, University of Colorado, CO, USA [3]Wright State University, Dayton, OH, USA [4]University of Michigan, Ann Arbor, MI, USA [5]Laboratoire atmosphères, milieux et observations spatiales (LATMOS)/CNRS, Paris, France *contact: mgacesa@ssl.berkeley.edu

1. Escape flux from in-situ measurements

Abstract. Dissociative recombination (DR) of photoionized O_2^+ with electrons in the upper atmosphere of Mars produces translationally superthermal O atoms capable of overcoming martian gravitational potential and escaping into space. This process is known as **photochemical escape** and found to be one of the major escape mechanisms presently (and formerly) active on Mars. MAVEN is the first spacecraft capable of measuring in-situ data from which O escape rates can be constructed.

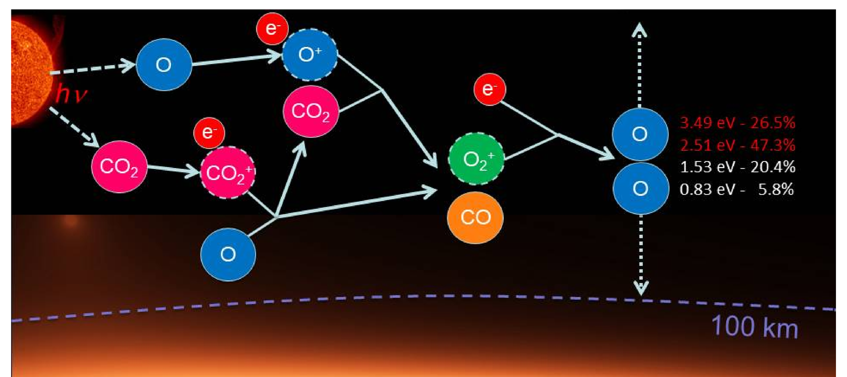

Fig. 1. Cartoon of photochemical escape mechanism

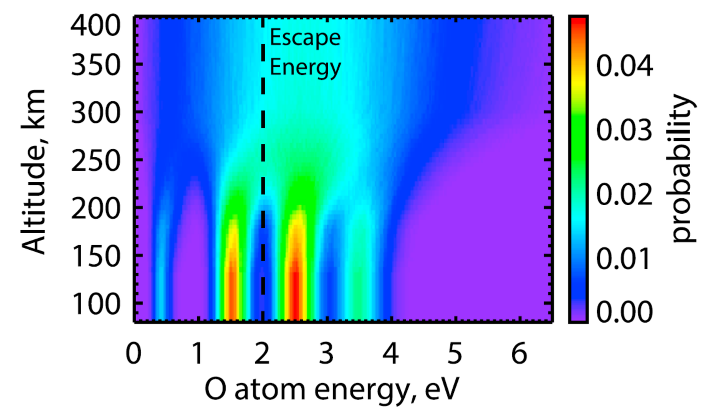

Fig. 2. Profile of hot O produced by DR of O_2^+.

MAVEN can constrain photochemical escape of oxygen from Mars using:

1) **In-situ measurements**. Rates of hot oxygen production are calculated using measurements of **electron temperature** and **density** (LPW instrument) and **ion temperature** and **density** (STATIC and NGIMS), while escape probabilities are calculated with **neutral densities** measured by NGIMS.

2) **Altitude profiles of 130.4 nm oxygen emission** measured up to ~4,000 km by the Imaging Ultraviolet Spectrograph (IUVS) can be fit to a model of photochemical escape to constrain escape fluxes.

3) **Energetic oxygen pickup ions** from the dayside oxygen exosphere that can be detected by the Solar Energetic Particle (SEP) instrument (E>70 keV), also allowing escape fluxes to be estimated.

The three methods give similar escape rates **~6-9 x 10^{25} s^{-1}** for the first 6 months of MAVEN data when solar EUV was comparatively high, but thereafter diverge, with the *in situ* method giving substantially lower fluxes than the other two methods.

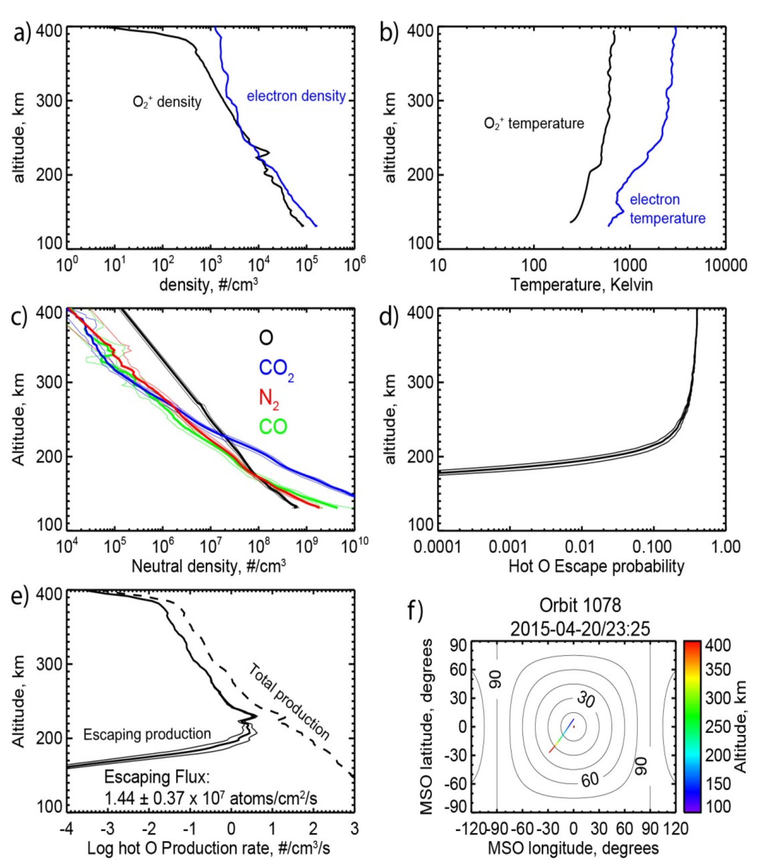

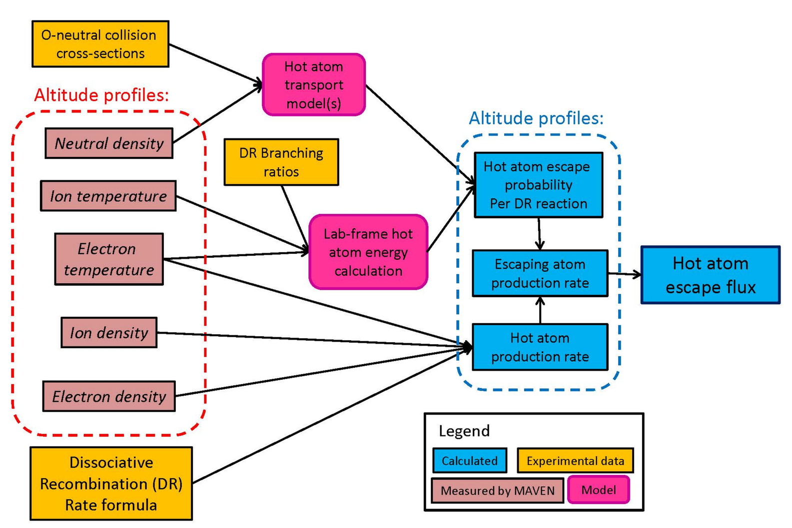

2. Data coverage

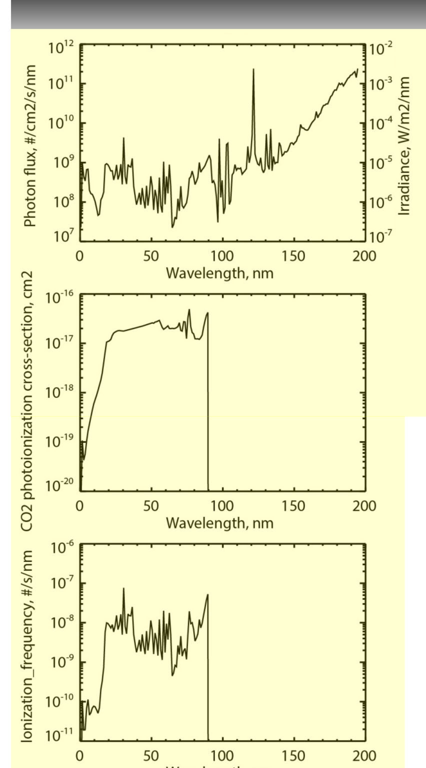

Fig. 3 (left) explains how we convert EUV irradiance to ionization frequency. The top panel shows an example of the EUV irradiance spectrum at Mars derived by the FISM model [Thiemann et al., 2016] and corresponding photon flux. The third panel shows CO2 photoionization cross section. The fourth panel shows differential ionization frequency, i.e. the product of proton flux and photoionization cross-section.

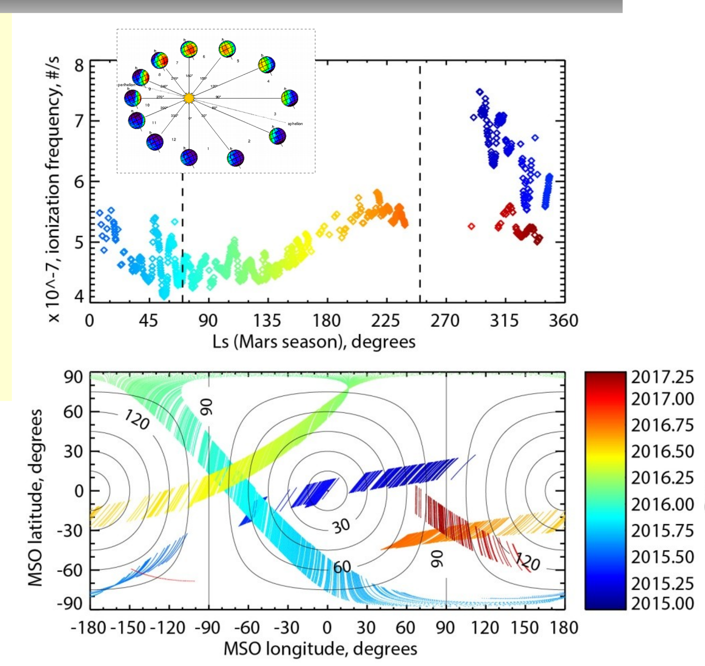

Fig. 4. (right) Data coverage in this study. ***Top:*** CO2 ionization frequency (see figure 4) decreases by ~40% with time as Mars moves further from the sun toward and past aphelion. ***Bottom:*** spacecraft location below 250 km in Mars-Solar-Orbital (MSO) coordinates. Missing data is due to:

- High spacecraft potentials: e^- temp. unreliable
- NGIMS instrument resets
- Solar conjunction

3. Variability of O escape fluxes

Derived O escape fluxes were found to depend on:

Solar Zenith Angle: escape fluxes don't show any dependence on SZA when SZA <95°. However, we see a dawn-dusk asymmetry.

Season/solar cycle: much higher escape fluxes at the start of 2015, just following perihelion. As Mars moves further from the sun and solar activity weakens, escape fluxes decrease by a factor of 2-3.

Crustal magnetic fields: no detectable dependence on the dayside, as expected. Nightside shows a slight hint of lower fluxes when fields are stronger, consistent with closed field loops retarding electron impact ionization

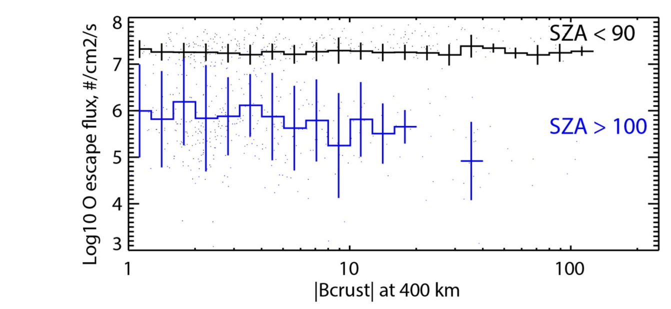

Derived escape fluxes are shown as a function of crustal magnetic field strength at 400 km.

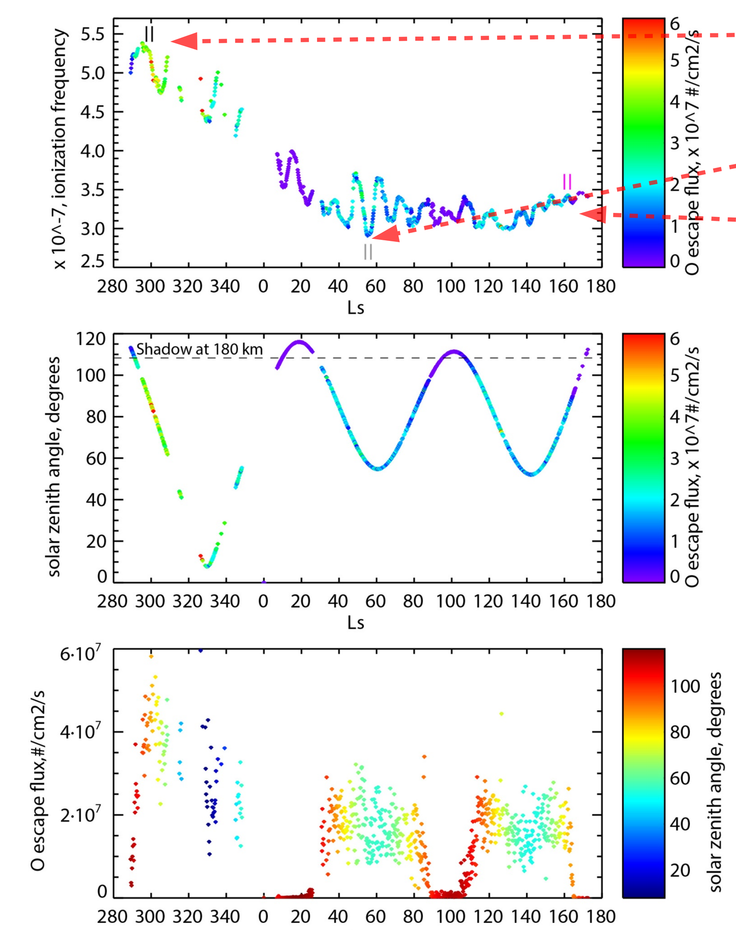

Derived escape fluxes are shown as a function of SZA, season, and photoionization frequency.

4. EUV dependence at the present epoch

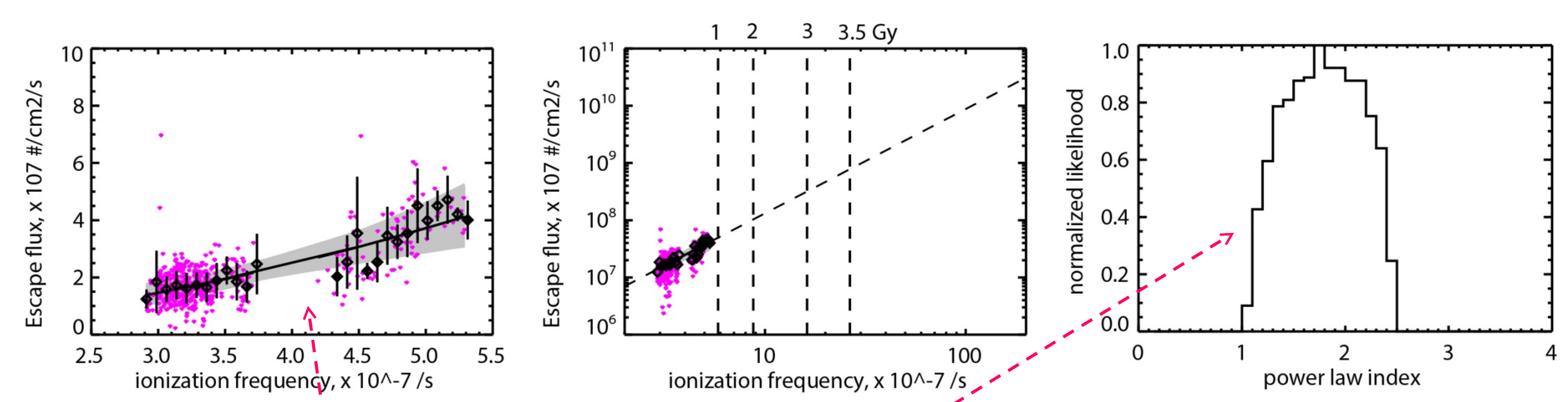

Positive dependence of dayside escape flux on ionization frequency. Best fit (power law): 1.8 ± 0.7

Modern-day ionization frequencies (since 1947): ~50% higher than those seen by MAVEN. *Courtesy of FISM-M (Thiemann et al., 2016).*

We can reconstruct global escape rates over the last 70 years: Range is 0.5-20 x 10^{25} O atoms s^{-1}. Average is 3.0 ± 1.8 x 10^{25}.

Effect of cross-sections. 40% lower assumed O-CO_2 collision cross-section gives ~40% higher escape flux.

However:
Ratio of cross-sections: 1.67
Ratio of escape fluxes: 1.38
Disagreement with Cravens *et al.* [2016]

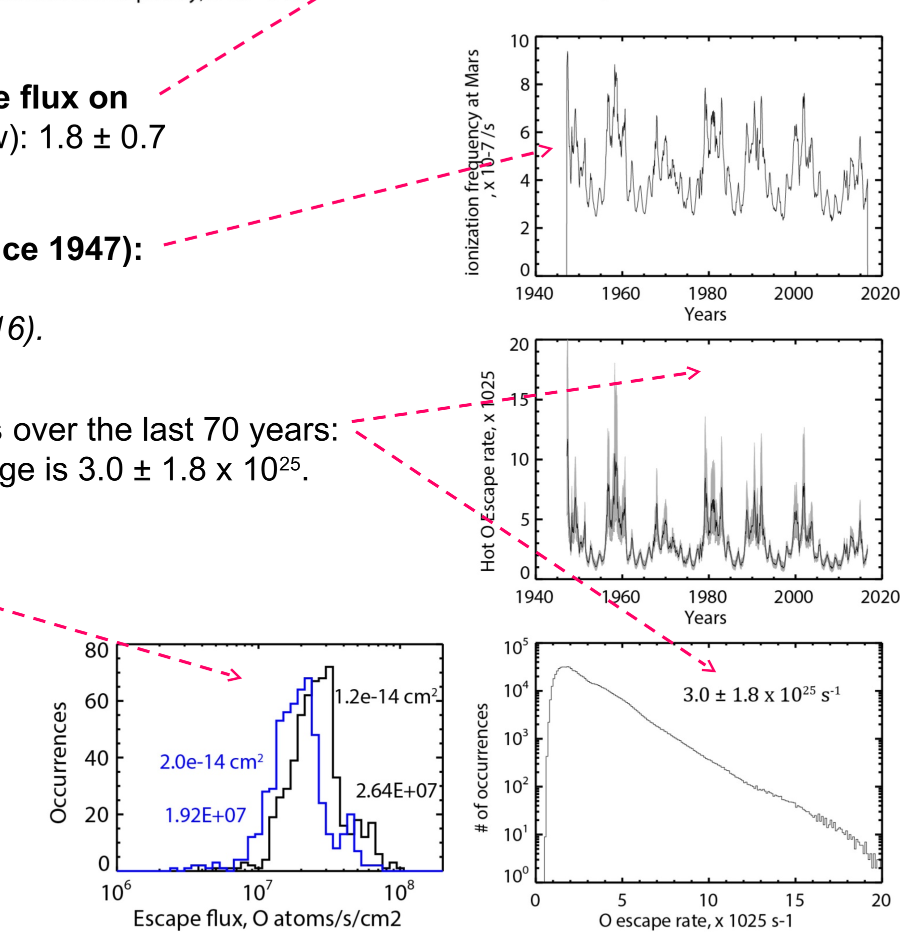

5. Example seasonal variations (3 periods)

Black curves: post-perihelion, mid-northern latitudes, high EUV, pre-dusk

Gray curves: almost aphelion, mid-southern latitudes, low EUV, late morning

Pink curves: northern autumn equinox, mid-northern latitudes, medium-low EUV, dawn

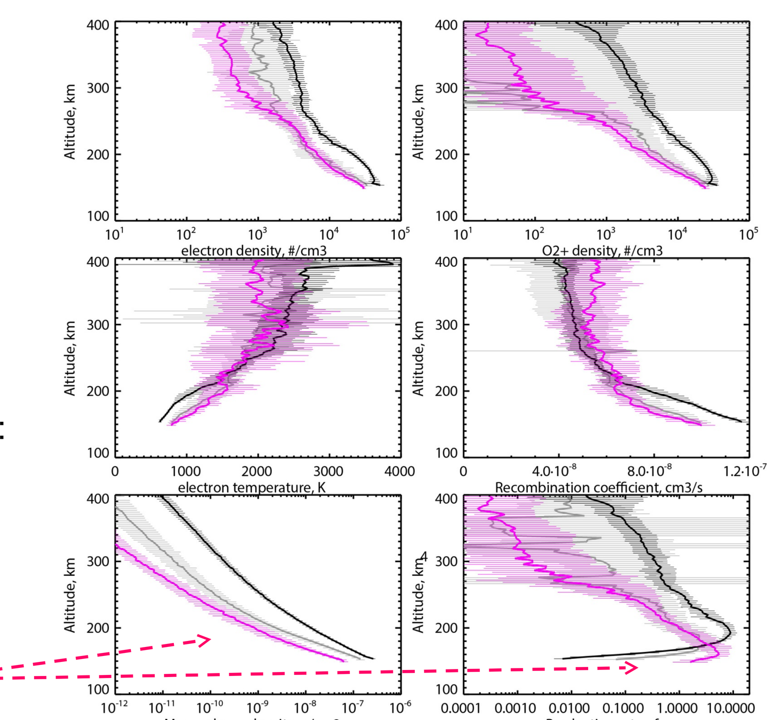

Production of escaping O atoms at altitude *z* a function of:

- Electron and ion density (positive)
- Electron temperature (negative)
- Column density of atmosphere above altitude *z* (negative)

To first order, atmospheric density doesn't matter: as neutral atmosphere gets thicker, ionization and escape move upwards.

But atmospheric composition does matter:

- Particularly near the exobase, where most escaping flux is produced.
- O, CO_2, N2, CO have different collision cross-sections
- Affects the relative amounts of CO_2^+, O^+ and O_2^+.
- Earlier epochs had different compositions

Interval	1 (Black)	2 (Gray)	3 (Pink)
Dates	2015-02-25 to 2015-03-01	2015-10-13 to 2015-10-19	2016-05-29 to 2016-06-03
Ls	297°-301°	54°-57°	160°-163°
IAU Latitude	31°-34° North	34°-39° South	38°-42° North
MSO Latitude	22°-24° North	48°-55° South	13°-17° North
SZA	85° to 92°	56° to 59°	78° to 86°
Local time	16.7-17.1	11.2 - 11.8	6.0-6.5
Ioniz. freq., 10-7 #/s	5.24 ± 0.07	2.94 ± 0.04	3.41 ± 0.02
O escape flux (x107 /cm2/s)	**4.3±0.6**	**1.3±0.4**	**1.6±0.5**

6. Non-thermal escape via collisions

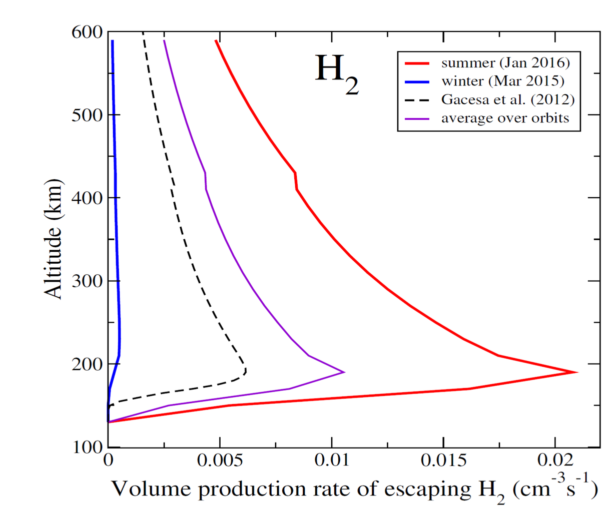

Escaping neutral OH: state-to-state profile

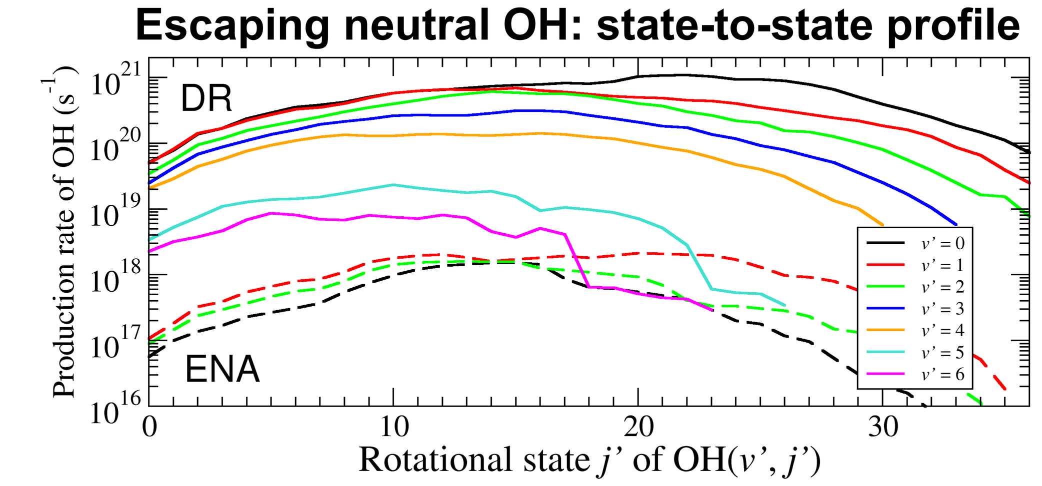

We performed MC simulations of collisions of precipitating solar wind ENAs (H, He) with atmospheric gasses in the Martian atmosphere. DR rates were calculated from hot electron and O_2^+ distributions given in Fox & Hac (Icarus, 204, 527 (2009)).

Significant seasonal differences (20x) in the predicted non-thermal escape rates of H_2, HD and He. The escape rates of H_2 are ~2-4x larger than in Gacesa *et al.*, GRL (2012) due to revised cross sections and added hot O production mechanisms.

Production rates of OH about 10% of H_2 and 0.1% of H. Vibrational states up to v' = 6 populated; we can expect several Meinel bands in emission.

Inputs

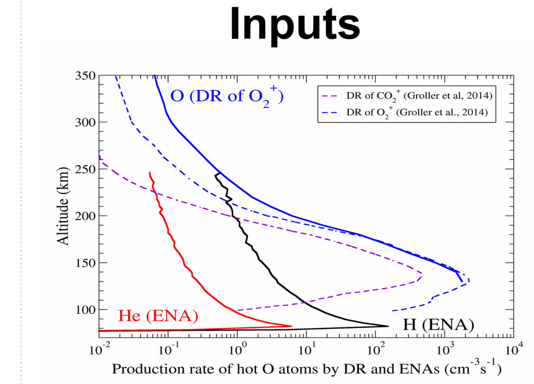

Altitude profile of the O produced by the DR and ENAs (from MC simulations of precipitating hot H and He atoms).

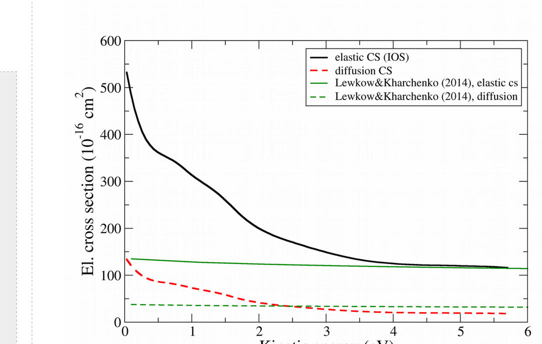

New QM elastic state-to-state cross sections evaluated using MOLSCAT code for energies up to 5 eV. Above 2 eV good agreement with Lewkow & Kharchenko (2014).

7. Conclusions & Future Directions

Escape rates in the modern epoch. O escape from O_2^+ dissociative recombination are expected to range from 10^{25} to 10^{26} atoms/s, averaging about 3 x 10^{25}.

O-CO_2 cross-section is the biggest uncertainty. Nailing this down is essential to understanding historical loss of oxygen. Our early calculations promise stronger escape*.

EUV dependence. We are trying to narrow the spread in power law exponents with more data.

Non-thermal escape of atoms/molecules need to be better understood to increase confidence.

Climate evolution: Difficult to get more than **~150 mbar** of escape of O over 3.5 Gyr?

Must combine with other instruments and missions for consistent & reliable estimate of photochemical escape.

References:

Lillis, R. *et al.* (2017), Photochemical escape of oxygen from Mars: First results from MAVEN in situ data, J. Geophys. Res., doi:10.1002/2016JA023525.

Cravens, T., *et al.* (2016), Hot oxygen escape from Mars: Simple scaling with solar EUV irradiance, J. Geophys. Res. 122, 1102; doi:10.1002/2016JA023461

Thiemann, E., P. Chamberlin, F. Eparvier, T. Woods, S. Bougher, and B. Jakosky (2016), The MAVEN/EUVM Level 3 Spectral Irradiance Model: Algorithms and Results, J. Geophys. Res.

Gacesa, M., Zhang, P., Kharchenko, V. (2012), Non-thermal escape of molecular hydrogen from Mars, Geophys. Res. Lett. 39, L10203; doi:10.1029/2012GL050904

Gacesa, M., Lewkow, N., Kharchenko, V. (2017), Non-thermal production and escape of OH from the upper atmosphere of Mars, Icarus 284, 90; doi: 10.1016/j.icarus.2016.10.030

Kharchenko, V., A. Dalgarno, B. Zygelman, and J. H. Yee (2000), Energy transfer in collisions of oxygen atoms in the terrestrial atmosphere, J. Geophys. Res., 105(24), 24899-24906, doi:10.1029/2000JA000085.

Lewkow, N. R., Kharchenko, V. (2014), Precipitation of energetic neutral atoms and induced non-thermal escape fluxes from the Martian atmosphere, Astrophys. J. 790, 98; doi: 10.1088/0004-637X/790/2/98